Green Chemistry

PAPER

View Article Online
View Journal

Cite this: DOI: 10.1039/d6gc00678g

Engineered microbial catalyst for simultaneous depolymerization and upcycling of polycaprolactone

Saint Moon Kim,[a,b] Yoonjoo Seo,[a] Renjing Jiang,[a] Linrui Tan,[b] Linduo Zhao,[d,e] John W. Scott,[d] Yong-Su Jin[b,c] and Na Wei *[a,b]

Plastic waste is a pressing global challenge. Although end-of-life plastics have long been regarded as an environmental burden, they also represent a vast yet underutilized carbon resource that could be redirected toward chemical production rather than discarded. Here we report an engineered microbial catalyst, PCL-DU, which enables one-pot biocatalytic depolymerization and upcycling of the plastic poly(ε-caprolactone) (PCL) into the high-value chemical adipic acid. PCL-DU integrates a cell surface catalytic depolymerization module based on curli nanofiber surface display of cutinase for extracellular PCL hydrolysis, and an intracellular biocatalytic cascade that converts the released monomer 6-hydroxyhexanoic acid (6-HHA) to adipic acid. This dual-functional microbial catalyst achieved complete one-pot conversion of PCL film to adipic acid under optimal conditions. In fed-batch operation, PCL-DU demonstrated catalytic robustness, maintaining activity over 9 days without the requirement for inducers or antibiotics, producing 12.07 ± 0.07 g adipic acid per L with a yield of 0.83 ± 0.00 g adipic acid per g PCL. Furthermore, we demonstrated the applicability of PCL-DU biocatalyst on real-world PCL products, achieving a conversion rate of 0.96 g adipic acid per L per day and a yield of 0.81 g adipic acid per g PCL. The recovered adipic acid was successfully polymerized into nylon-6,6, establishing a complete upcycling pathway from plastic waste to industrial polymer. In all, the dual-functional microbial catalyst achieved simultaneous biocatalytic depolymerization and conversion of PCL into high-value chemical adipic acid by spatially integrating extracellular enzymatic plastic depolymerization with intracellular biotransformation. This work provides a novel biocatalytic platform for advancing sustainable recovery and upcycling of plastic carbon.

Received 31st January 2026,
Accepted 9th April 2026

DOI: 10.1039/d6gc00678g

rsc.li/greenchem

Green foundation

1. This work advances the field of green chemistry by establishing a novel dual-functional microbial catalyst that enables simultaneous biocatalytic depolymerization and value-added biotransformation of plastic waste into a high-value chemical (adipic acid) in one pot, addressing key sustainability challenges in plastic carbon valorization.
2. The engineered microbial catalyst achieved complete conversion of poly(ε-caprolactone) (PCL) into adipic acid with a yield of 0.83 g g^{-1} PCL under mild conditions, bypassing enzyme purification and intermediate separation while improving efficiency through *in situ* monomer consumption.
3. Future research could make the system greener by developing genome-integrated stable microbial systems to improve cost-effectiveness and minimize potential environmental risks for scalable industrial applications. The modular microbial platform developed in this study can further be extended to broader classes of plastics to address the grand challenge of plastic waste management within a circular bioeconomy framework.

[a]*Department of Civil and Environmental Engineering, University of Illinois at Urbana-Champaign, 3221 Newmark Civil Engineering Laboratory, 205 N. Mathews Avenue, Urbana, Illinois 61801, USA. E-mail: nawei2@illinois.edu*
[b]*Carl R. Woese Institute for Genomic Biology, University of Illinois at Urbana-Champaign, Urbana, Illinois 61801, USA*
[c]*Department of Food Science and Human Nutrition, University of Illinois at Urbana-Champaign, Urbana, Illinois 61801, USA*
[d]*Illinois Sustainable Technology Centre, Prairie Research Institute, University of Illinois at Urbana Champaign, Champaign, IL 61820, USA*
[e]*Illinois State Water Survey, Prairie Research Institute, University of Illinois at Urbana Champaign, Champaign, IL 61820, USA*

Introduction

The extensive use of plastic commodities inevitably generates large amounts of plastic waste, posing serious challenges to ecosystems and humans health.[1–3] Efforts to reduce the environmental impact of plastics have spurred the development of biodegradable alternatives.[4] A promising biodegradable plastic of growing use is poly(ε-caprolactone) (PCL). PCL is a semicrystalline aliphatic polyester widely applied in biomedical devices, packaging, agricultural films,

and additive manufacturing, due to its favorable physicochemical properties such as low melting point, low viscosity, and high thermal processability.[5–7] However, despite being classified as a biodegradable plastic, PCL is still prone to accumulate in the environment and its degradation under natural conditions is notably slow due to its hydrophobic and semi-crystalline structure.[8–11] For example, PCL fragments have been detected in nearly 10% of net samples from the Mediterranean Sea, which provides clear evidence of its poor degradability in the natural environment.[12] Degradation of PCL proceeds slowly under landfill conditions, and even under composting conditions, only minimal surface erosion and weight loss are observed over two months.[10,11]

While end-of-life plastics have often been regarded as an environmental burden, they also represent a vast and underexploited reservoir of carbon which could be redirected toward sustainable biomanufacturing rather than discarded.[13] Conventional plastic waste treatment methods such as landfilling and incineration not only generate pollution but also fail to valorize hydrocarbon from plastic materials,[14] whereas mechanical recycling methods typically result in reduced product quality (downcycling) and have high energy demands.[15] In contrast, plastic upcycling aims to catalytically depolymerize polymers into intermediates that can be further converted to high-value products.[15,16] PCL plastic can be depolymerized into 6-hydroxyhexanoic acid (6-HHA), which is a chemically versatile intermediate for the synthesis of value-added compounds. One particularly attractive target is adipic acid, a key precursor for the industrial production of nylon-6,6, plasticizers, polyurethanes, and resins.[17] The global demand for adipic acid exceeds five million metric tons annually and is projected to grow by 50% before 2030.[18,19] Current production of adipic acid rely heavily on chemical synthesis from petroleum-derived feedstocks *via* nitric acid oxidation of cyclohexanol or cyclohexanone, a process that is energy-intensive and releases potent greenhouse gas nitrous oxide.[17] Therefore, upcycling of PCL into adipic acid represents a promising and sustainable alternative to conventional petrochemical synthesis, which could offer advantages in valorizing plastic waste while reducing greenhouse gas emissions and fossil resource dependency.

Biocatalysis provides an attractive and promising route for plastic depolymerization and upcycling, but key challenges exist in the development of efficient and economically viable processes. Enzymatic depolymerization has advantages of high efficiency under mild conditions, lack of toxic byproducts, and low energy and chemical demands,[16,20] Prior studies have demonstrated PCL depolymerization into 6-HHA by using lipases and cutinases.[21–23] However, the use of free enzymes has inherent limitations including the single-use, high production costs, and poor stability under industrial conditions.[20] Another critical issue is potential inhibition of enzyme activity by products from plastic depolymerization. For example, the accumulated 6-HHA been shown to inhibit the enzyme CalB activity during PCL depolymerization.[22] The problem associated with product accumulation requires downstream separation and transfer steps, which can lead to yield loss, increased operational complexity, and a higher risk of contamination.[24]

To overcome these limitations, we aimed to develop a renewable biocatalytic system capable of simultaneous plastic depolymerizing and conversion. We designed a new type of dual-functional microbial catalyst to depolymerize PCL and convert the resulting monomer 6-HHA into adipic acid in one pot. Our design integrates two functional modules: a cell surface catalytic depolymerization module displaying the plastic-degrading enzyme, and an intracellular bioconversion module containing the biocatalytic cascade pathway to convert the monomer 6-HHA to adipic acid. For cell surface depolymerization module, we employed the Biofilm-Integrated Nanofiber Display (BIND) platform in *Escherichia coli*.[25] The BIND platform enables display of target proteins on the curli, extracellular amyloid nanofibers on the bacterial surface. By genetically fusing a PCL-depolymerizing enzyme to the curli building block, CsgA subunit, the enzyme is expressed and autonomously displayed along with the curli formation (Fig. 1). The inherent affinity of curli nanofibers for solid surfaces[25,26] can benefit interaction between the displayed enzyme and plastic substrate. In our prior study, we showed that PETase displayed *via* the BIND system enabled efficient depolymerization of polyethylene terephthalate (PET).[20] For bioconversion module, we sought to engineer a heterologous pathway consisting of 6-HHA dehydrogenase and 6-oxohexanoic acid dehydrogenase for the conversion of 6-HHA into adipic acid (Fig. 1). This dual-function microbial catalyst design will have two major benefits. On one hand, the cell surface module ensures enzyme functionality and renewability through automatic surface display, eliminating the need for protein purification. On the other hand, establishing the 6-HHA-to-adipic acid conversion pathway in the same cell can facilitate mass flux from the monomer toward the product. By consuming the monomer immediately as it is produced, the approach can bypass the need for intermediate separation and mitigate feedback inhibition, thus improving overall catalytic efficiency and cost-effectiveness for plastic upcycling.

In this study, we constructed and characterized the engineered microbial catalyst PCL-DU and demonstrated efficient upcycling of PCL into adipic acid in a one-pot process (Fig. 1). The biocatalyst PCL-DU displays *Fusarium solani* cutinase, a well-characterized PCL-degrading enzyme[27] on curli nanofibers, and expresses the functional bioconversion pathway *via* co-expression of 6-HHA dehydrogenase (ChnD) and 6-oxohexanoic acid dehydrogenase (ChnE) from *Acinetobacter strain SE19*.[28] We characterized the kinetics and functionality of depolymerization module and bioconversion module, optimized key reaction conditions for simultaneous depolymerization and upcycling, and evaluated the catalytic performance of PCL-DU in fed-batch fermentation to enhance yield, titer, and productivity. Moreover, we demonstrated efficient biocatalytic conversion of real-world PCL products to adipic acid, which was subsequently polymerized into nylon-6,6, thereby establishing a complete upcycling pathway from waste to valuable industrial product. Overall, PCL-DU represents the first demonstration of a living catalyst capable of simultaneous depolymerization and upcycling of PCL into high-value chemical adipic acid.

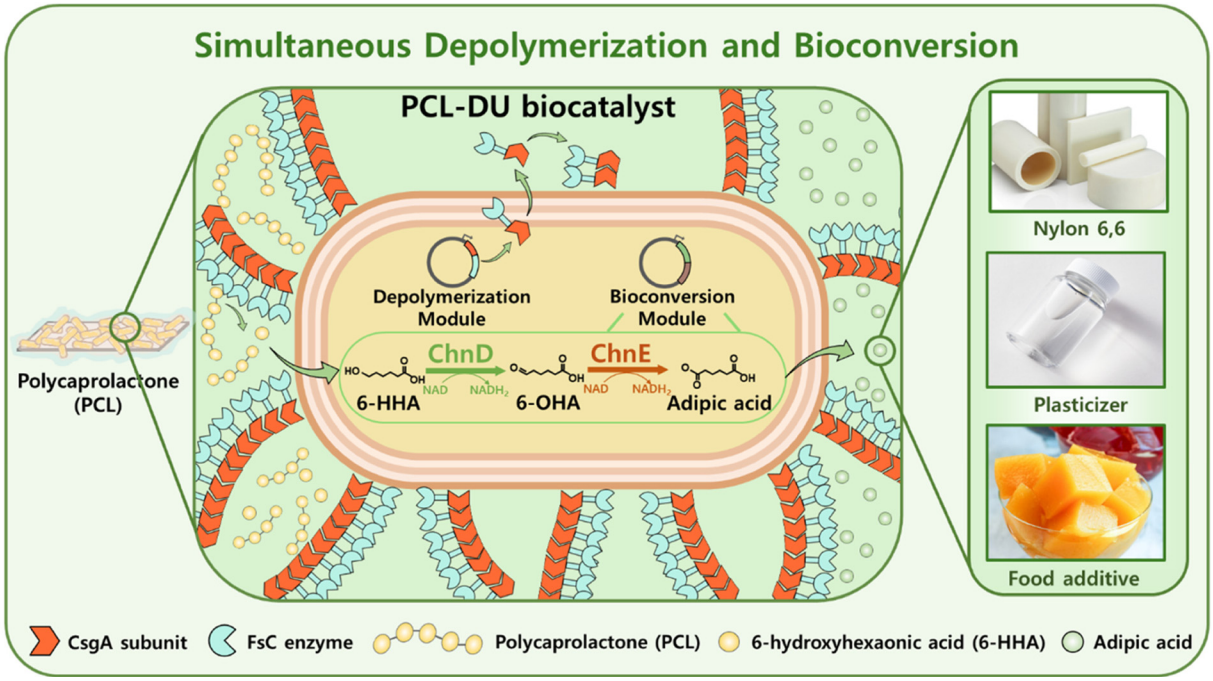

Fig. 1 Schematic diagram illustrating simultaneous depolymerization and conversion of polycaprolactone (PCL) into adipic acid using PCL-DU biocatalyst. The depolymerization module expresses FsC fused to CsgA, producing functionalized curli fibers on the cell surface for extracellular PCL depolymerization. Concurrently, the bioconversion module expresses the ChnD and ChnE enzymes that catalyze the sequential oxidation of 6-hydroxyhexanoic acid (6-HHA) to 6-oxohexanoic acid (6-OHA) and finally to adipic acid. The released 6-HHA from PCL depolymerization is taken up by PCL-DU biocatalyst and converted through the bioconversion pathway, resulting in adipic acid. Adipic acid is a key precursor for producing nylon-6,6, plasticizers, and food additives.

By integrating depolymerization and value-added biotransformation within a single microbial system, this work introduces a novel biocatalytic strategy for circular plastic technologies.

Experimental section

Strains, plasmids and culture conditions

E. coli TOP 10 was used in cloning work for constructing the pBbE1a-CsgA-FsC plasmid and was incubated at 37 °C in Luria broth (LB) medium with 100 μg mL^{-1} ampicillin. *E. coli* JM109 was utilized for pTac15K-ChnDE plasmid construction and cultured in LB medium with 50 μg mL^{-1} of zeocin (LBZ). *E. coli PHL628 ΔcsgA* was used as the expression host for the one-pot microbial cell factory and was cultured in YESCA (1 g L^{-1} yeast extract, 10 g L^{-1} casamino acids) medium to support curli production.[29] The detailed microbial strains and plasmids used in this study are listed in Table 1.

PCL film preparation

Commercial PCL powder (particle size <74 μm) was purchased from Nanochemazone (Leduc, AB) and used to prepare PCL films *via* the solvent casting method. The PCL powder has a weight-average molecular weight (M_w) of 85 000 g mol^{-1}, a number-average molecular weight (M_n) of 47 500 g mol^{-1}, and a polydispersity index (PDI) of 1.79. A total of 2.682 g of PCL powder was dissolved in 36 mL of chloroform (5 wt%) and cast into a glass Petri dish. The solution was dried in a fume hood for 24 hours, then washed three times with distilled water (DW) and dried at 37 °C for 24 hours.[30]

Construction of PCL depolymerizing and bioconversion modules

The *Fusarium solani* cutinase and *ChnD*/*ChnE* (*ChnDE*) genes were codon-optimized for *E. coli* and synthesized by Twist Bioscience (South San Francisco, CA). The primers used in this study are listed Table S1. The *FsC* gene was PCR-amplified using Primer 1/Primer 2 and ligated into the pBbE1a-CsgA plasmid *via* BamHI/XhoI digestion (Table S1). The resulting construct was transformed into *E. coli* Top10 and selected on LB agar plate. For *ChnDE*, the gene was amplified with Primer 3/Primer 4 and subsequently cloned into the pTac15K plasmid *via* EcoRI/PstI sites (Table S1). The resulting plasmid was transformed into *E. coli* JM109 and selected on LB agar plate supplemented with ampicillin (LBA). To enable co-transformation of pTac15K-ChnDE and pBbE1a-CsgA-FsC, the kanamycin resistance marker in pTac15K-ChnDE was replaced with a zeocin resistance marker. The antibiotic marker replacement was performed using Gibson assembly, wherein the pTac15K-ChnDE backbone and the zeocin resistance cassette were PCR-amplified with Primer 5/Primer 6 and Primer 7/Primer 8, respectively (Table S1). The final construct, pTac15K-ChnDE with a zeocin marker, was transformed into *E. coli* JM109 and selected on LBZ plate.

Table 1 Strains and plasmids used in this study

Plasmids and strains	Description	Ref.
Plasmids		
pBbE1a-CsgA	A backbone plasmid for constructing pBbE1a-CsgA-FsCc	20
pBbE1a-CsgA-FsC	A backbone plasmid for constructing pBbE1a-CsgA-FsC	This study
pTac15K	A backbone plasmid for constructing pTac15K-ChnDE	NovoPro Bioscience Inc.
pTac15K-ChnDE	pTac15K with gene encoding ChnD and ChnE	This study
pTac15K-ChnDE (Zeo)	pTac15K-ChnDE with Zeocin marker	This study
Strains		
E. coli DH5α	A host strain for gene cloning	New England Biolabs
E. coli JM109	A host strain for gene cloning	Zymo Research
E. coli PHL628	A host strain for BIND system	20
PCL-D		
E. coli PHL628 with pBbE1a-CsgA-FsC	*E. coli* PHL628 with PCL depolymerization unit	This study
PCL-U		
E. coli PHL628 with pTac15K-ChnDE (Zeo)	*E. coli* PHL628 with PCL bioconversion unit	This study
PCL-DU		
E. coli PHL628 with pBbE1a-CsgA-FsC and pTac15k-ChnDE (Zeo)	*E. coli* PHL628 with PCL depolymerization unit and 6-HHA bioconversion unit	This study

Recombinant plasmids were extracted using the QIAprep Spin Miniprep Kit (Qiagen Inc.) following the manufacturer's instructions. The purified plasmids were subsequently transformed into *E. coli* PHL628 to generate the following recombinant strains: *E. coli* PHL628 harboring pBbE1a-CsgA-FsC (PCL-D), which functions as the depolymerization module; *E. coli* PHL628 harboring pTac15K-ChnDE (PCL-U), which functions as the bioconversion module; and *E. coli* PHL628 harboring both pBbE1a-CsgA-FsC and pTac15K-ChnDE (PCL-DU), which integrates both depolymerization and bioconversion modules in a single strain. The transformants were selected on LBA, LBZ, and LB agar plates supplemented with ampicillin and zeocin (LBAZ), respectively.

Congo red binding assay

Congo red (CR) binding assay was performed for confirmation and semi-quantification of amyloid nanofiber formation.[20] CR is a dye which specifically binds to the amyloid structure of *E. coli* curli fibers, making it a widely used method to assess curli formation. Briefly, induced *E. coli* cells were washed twice with glycine–NaOH buffer (pH 9) and resuspended in 1 mL PBS buffer to an OD_{600} of 3.0. CR was added at a final concentration of 0.025 mM, and the samples were incubated at 25 °C with shaking at 260 rpm for 10 min. Cells were then collected by centrifugation at 16 000*g* for 5 min, and the absorbance of the supernatant was measured at 490 nm. The absorbance was normalized by subtracting the blank (PBS containing CR without cells) and dividing by the OD_{600} value. Wild-type *E. coli* PHL628 was used as a negative control, and all measurements were performed in triplicate.

Enzyme activity assay

The hydrolytic activity of recombinant strains was quantified using a standard *p*-nitrophenyl butyrate (*p*-NPB) hydrolysis assay. Briefly, 10 μL of induced cells (OD_{600} = 3), 182 μL of PBS buffer (pH 7.0), and 8 μL of 2 mM *p*-NPB solution dissolved in DMSO were added into 96-well microplates and gently mixed. The reaction was monitored by measuring absorbance at 405 nm every 2 min for a total of 30 min using a microplate reader (Synergy 2, Biotek) at 30 °C with continuous shaking. Enzyme activity was calculated from the initial catalytic rate based on the linear slope of reaction curve, using a *p*-nitrophenol (*p*-NP) standard curve. Wild-type *E. coli* PHL628 was used as a negative control. One unit (U) of enzyme activity was defined as the amount of enzyme required to produce 1 mmol of *p*-NP per minute (U = mmol *p*-NP per min). All measurements were performed in triplicate.

PCL depolymerization experiments

The PCL hydrolytic activity of PCL-D and PCL-DU were evaluated using PCL film as a substrate. Initially, PCL-D or PCL-DU was cultured overnight at 30 °C with shaking at 250 rpm in LB medium supplemented with antibiotics. The overnight culture was inoculated into fresh YESCA medium with antibiotics at a 1 : 100 dilution ratio and incubated until an OD600 reaches 0.6. At this point, induction was initiated with 0.8 mM IPTG and continued for 22 h at 26 °C with shaking at 60 rpm. Following induction, cells were harvested by centrifugation at 4000*g* for 5 min, washed twice, and resuspended in 50 mM glycine–NaOH buffer (pH 9.0). A reaction mixture containing 5 U of cells, 50 mg (±10%) of PCL film, and 25 mL of 50 mM glycine–NaOH buffer (pH 9.0) was prepared in 125 mL flasks and incubated at 37 °C. All experiments were conducted in triplicate. Wild-type *E. coli* PHL628 was used as a negative control. To prepare samples for field emission scanning electron microscopy (FE-SEM), PCL-D experiments were conducted under the same conditions. Flasks were sacrificed every 4 h, and residual PCL films were collected using a 100 μm cell strainer. The films were washed twice with distilled water, dried, and prepared for imaging.

Conversion of 6-HHA to adipic acid

To confirm the successful establishment of the 6-HHA bioconversion pathway, experiments were conducted using the PCL-U biocatalyst with different concentrations of 6-HHA (0–10 g L^{-1}). PCL-U was pre-cultured overnight at 37 °C in LBZ medium with shaking at 250 rpm. 6-HHA (0–10 g L^{-1}) was added to the LBZ medium, and the pH was adjusted to 7.0 using 1 M NaOH. The overnight culture was then inoculated into LBZ medium at a 1 : 100 dilution ratio and further grown until the OD600 reached 0.6. At this stage, IPTG was added to a final concentration of 0.8 mM, to initiate the conversion reaction. A control using wild-type *E. coli* PHL628 was included, and all experiments were conducted in triplicate. The same experimental setup was also carried out with the PCL-DU biocatalyst using 2.5 g L^{-1} of 6-HHA.

One-pot PCL depolymerization and upcycling

The performance of PCL-DU was evaluated using PCL film as a substrate. Initially, PCL-DU was cultured overnight and inoculated into fresh YESCA medium with antibiotics at a 1 : 100 dilution. When OD600 reached 0.6, 0.8 mM IPTG was added and incubated 22 h at 26 °C with shaking at 60 rpm. Following induction, 5 U of PCL-DU was prepared in 25 mL of YESCA medium supplemented with 10 g L^{-1} of $CaCO_3$, antibiotics and 50 mg (±10%) of PCL film and incubated at 37 °C with shaking at 250 rpm. All experiments were conducted in triplicate.

The one-pot depolymerization and upcycling activity of PCL-DU toward PCL was optimized by varying agitation speed and incubation temperatures. Initially, PCL-DU was cultured overnight at 30 °C with shaking at 250 rpm in YESCA medium with antibiotics. The overnight culture was then diluted into 50 mL of fresh YESCA medium with 10 g L^{-1} of $CaCO_3$ and antibiotics in a 250 mL flask at a 1 : 100 dilution ratio and incubated until an OD600 reaches 0.6. At this point (defined as 0 h), IPTG (0.8 mM) and PCL film (40 mg ± 10%) were added to induce protein expression and initiate depolymerization. Cultures were induced at 26 °C with shaking at 60 rpm for 22 h. After induction, the same flasks were transferred to varying shaking speeds (0, 60, 100, and 250 rpm) and incubation temperatures (30 °C, 37 °C, and 42 °C) for continued incubation. Samples were collected at 24 h intervals, and all experiments were performed in triplicate to ensure reproducibility. A negative control without IPTG induction was also included.

Fed-batch PCL depolymerization and upcycling

Fed-batch PCL depolymerization and upcycling by the microbial catalyst were evaluated under three different conditions. PCL-DU was first cultured overnight at 30 °C with shaking at 250 rpm in YESCA medium with ampicillin and zeocin. Overnight cultures were diluted 1 : 100 into 800 mL of fresh YESCA medium with antibiotics and incubated overnight under the same conditions. The overnight cultures were then washed twice and prepared according to each experimental condition. For preparation of induced PCL-DU biocatalyst, overnight cultures of PCL-DU were reinoculated into 800 ml of fresh YESCA medium with ampicillin and zeocin and grown to an OD_{600} of 0.6, followed by induction with IPTG (0.8 mM) at 26 °C for 22 h. Induced cells were harvested, washed, and resuspended for subsequent experiments. The three conditions tested were: (i) PCL-DU cells in YESCA medium supplemented with antibiotics and IPTG (0.8 mM); (ii) PCL-DU cells in YESCA medium without antibiotics but with IPTG (0.8 mM); and (iii) PCL-DU biocatalyst in YESCA medium without antibiotics and IPTG. For all conditions, cultures were adjusted to a starting OD_{600} of 5 and supplemented with 10 g L^{-1} $CaCO_3$, after which PCL film (200 mg) was added. The flasks were incubated at 37 °C with shaking at 100 rpm. Additional PCL film was supplied on days 2 (200 mg) and 3 (100 mg), and 500 μL of 10× concentrated YESCA medium was supplemented every 24 h. Samples were collected at 12 h intervals, and all experiments were performed in triplicate.

Post-consumer PCL depolymerization and upcycling

A commercial PCL filament was used to fabricate a 3D-printed product (5 g; dimensions: 3.17 × 5.08 cm), which served as the substrate. PCL-DU was cultured overnight in YESCA medium with antibiotics at 30 °C with shaking at 250 rpm, harvested, washed, and resuspended to a starting OD_{600} of 5 in 200 mL of fresh YESCA medium supplemented with 10 g L^{-1} of $CaCO_3$ and antibiotics in a 1 L beaker. The beaker was incubated at 37 °C with shaking at 100 rpm, with 0.8 mM IPTG added at the start of incubation. 10× concentrated YESCA medium and antibiotics were supplemented every 24 h. Samples were collected every 12 h.

Adipic acid to nylon-6,6

To recover adipic acid, the culture medium was centrifuged at 7000 rpm for 10 min after PCL valorization, and the pH of the supernatant was adjusted to 9.0 using 1 M NaOH. Granular activated carbon (GAC, 10% w/v) was added, and the mixture was stirred for 1 h at room temperature. Following treatment, the suspension was centrifuged again at 7000 rpm for 10 min. The resulting supernatant was acidified to pH 2.0 using 1 M HCl, filtered through a 0.45 μm membrane filter, and concentrated by boiling. The concentrate was then placed on ice to initiate the crystallization of adipic acid. The precipitated adipic acid was redissolved in distilled water and subjected to a second round of GAC treatment under the same conditions. The final adipic acid precipitate was dried and stored in a desiccator until further use. To synthesize nylon-6,6, adipoyl chloride was first prepared by reacting 0.3 g of adipic acid with 1 mL of thionyl chloride ($SOCl_2$) in a 50 mL round-bottom flask at 80 °C for 1 h. The resulting adipoyl chloride (0.7 mL) was then dissolved in 20 mL of hexane. Separately, a solution containing 0.5 g of hexamethylene diamine (HMDA), 0.75 g of NaOH, and 25 mL of distilled water was prepared. The two solutions were carefully combined in a beaker without mixing, allowing interfacial polymerization to occur at the phase boundary, resulting in the formation of nylon-6,6. The same

procedure was also applied to nylon-6,6 synthesis using commercial adipic acid (≥99.5%, Sigma-Aldrich, USA).

Analytical methods for cell growth and product quantification

Cell density were monitored by measuring the optical density at 600 nm (OD600) using a UV-visible spectrophotometer (BioMate 3S; Thermo Fisher Scientific, USA). The concentrations of 6-HHA and adipic acid were analyzed using high-performance liquid chromatography (HPLC, Agilent 1200 Series; Agilent Technologies, USA) equipped with a refractive index detector and a Rezex ROA-Organic Acid H^+ 8% column (Phenomenex, CA). The mobile phase consisted of 0.005 M H_2SO_4, with a flow rate of 0.6 mL min^{-1}, and the column temperature was maintained at 50 °C. All samples were centrifuged at 13 000 rpm for 10 min and filtered through a 0.22 μm membrane prior to HPLC measurement.

FE-SEM analysis

The surface morphology of PCL films was analyzed using a field emission scanning electron microscope (Hitachi S-4800, Japan). The samples were washed with distilled water and dried at 37 °C overnight. The dried samples were then mounted, coated with Au/Pd for 20 s, and analyzed at an accelerating voltage of 2.0 kV.

Infrared analysis

To compare the synthesized nylon-6,6 with a standard reference, infrared (IR) spectra were acquired using a Thermo Scientific Nicolet™ iN10 MX microscope operated in attenuated total reflectance (ATR) mode. Small sample pieces (5–10 mm) were placed directly onto the germanium ATR crystal without further preparation, and three measurement spots were randomly selected across the sample surface. Spectra were collected in the mid-infrared region (4000–675 cm^{-1}) at a resolution of 4 cm^{-1} with 32 co-added scans to improve the signal-to-noise ratio. Background spectra were recorded prior to each measurement and automatically subtracted. The resulting spectra were processed using OMNIC™ software for baseline correction, normalization, and identification of characteristic absorption bands.

Pyrolysis-gas chromatography mass spectrometry

The synthesized nylon-6,6 and the standard reference were further analyzed for their chemical component by pyrolysis-gas chromatography-mass spectrometry (Py-GC-MS) using a Pyroprobe 5200 High-Pressure Pyrolyzer with thermal desorption and reactant gas operation, interfaced to a Shimadzu QP-2010 SE single quadrupole GC-MS. Approximately 5 mg of material was cut from each sample, placed into a quartz capillary tube, and loaded into the pyroprobe. Pyrolysis was carried out at 600 °C for 90 s. The GC injection port (split ratio 100 : 1) and transfer line were maintained at 300 °C. Separation was achieved on a Restek Rtx-5MS capillary column (30 m × 0.25 mm i.d., 0.25 μm film thickness) using helium as the carrier gas at a flow rate of 1.0 mL min^{-1}. The GC oven was initially held at 40 °C for 2 min, then ramped at 10 °C min^{-1} to 300 °C. Mass spectra were collected over an m/z range of 35–350 Da, with a scan rate of three scans per second and a dwell time of 300 ms. Blanks were run before and after each sample until a stable baseline was obtained.

TGA measurement

The thermal stability of nylon-6,6 was evaluated using a thermogravimetric analyzer (TGA Q50, TA Instruments, USA). Approximately 10 mg of sample was loaded into a platinum pan and analyzed from room temperature to 600 °C at a constant heating rate of 10 °C min^{-1}. The measurement was performed under a nitrogen atmosphere with a balance gas flow of 40 mL min^{-1} and a sample gas flow of 60 mL min^{-1}.

Differential scanning calorimetry analysis

Thermal transitions of adipic acid and nylon-6,6 were analyzed using a differential scanning calorimetry (DSC 2500, TA Instruments, USA). Approximately 5 mg of sample was sealed in an aluminum pan and subjected to a heating ramp from 30 °C to above its melting point at a rate of 10 °C min^{-1}. A cooling and reheating cycle were applied, and all thermal parameters were determined from the second heating cycle. The purity of adipic acid was analyzed using the TA Universal Analysis software, which calculates purity based on the slope at the melting onset according to the van't Hoff equation.

Results and discussion

Depolymerization module: functional display of cutinase on *E. coli* curli nanofibers

The PCL depolymerization module on the surface of *E. coli* was successfully constructed by displaying FsC on the curli nanofibers, yielding the strain PCL-D (Fig. 2A). The gene encoding the enzyme FsC was codon optimized and fused to the *csgA* gene. The fusion protein was expressed under the control of IPTG-inducible *trc* promoter (Fig. S1). *E. coli* PHL628 was selected as a host strain due to its genomic deletion of native *csgA* gene and an *ompR* mutation, which enhances its capability for curli biogenesis.[31] Successful display of FsC on *E. coli* curli nanofibers was confirmed through a combination of structural and functional assays. The Congo Red (CR) binding assay revealed a strong red coloration in PCL-D, whereas the control strain without curli expression did not bind CR and remained pale (Fig. S2). The PCL-D showed a 6.2-fold higher activity toward CR than the negative control (Fig. 2B), confirming that curli nanofibers were formed as designed in the engineered strain. The PCL-D biocatalyst exhibited a specific enzyme activity of 112.4 ± 11.5 U g^{-1} dry cell weight, whereas no detectable activity was observed in the negative control (Fig. 2C). These results confirmed that FsC was successfully displayed on the cell surface *via* curli fibers and functionally retained its enzymatic activity.

We next evaluated the capability of PCL-D for depolymerizing PCL film. When PCL film was incubated with the biocatalyst, the PCL-D cells effectively depolymerized 50 mg PCL film within

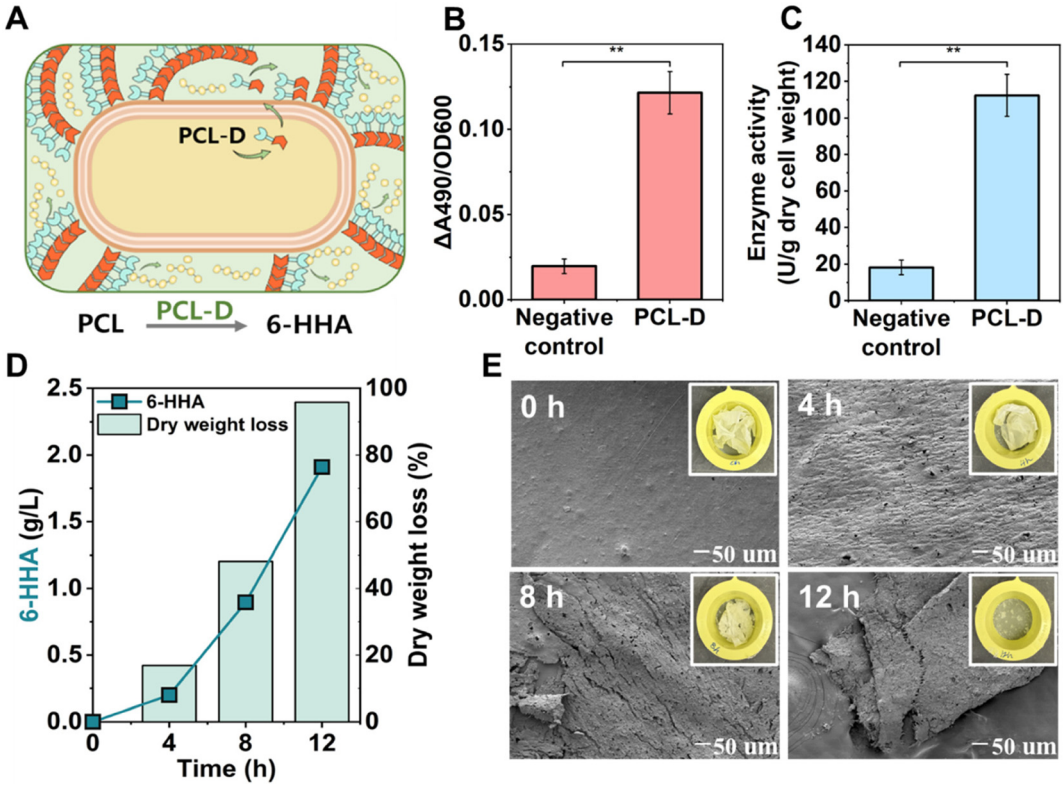

Fig. 2 Construction and characterization of PCL depolymerization module in the PCL-D biocatalyst. (A) Schematic diagram of PCL-D. Depolymerization module is expressed in PCL-D, in which FsC is fused with CsgA and displayed on the curli fibers, enabling the depolymerization of PCL into 6-HHA. (B) Congo red binding assay to evaluate curli formation. Congo red interacts with curli amyloid fibers, resulting in increased absorbance at 490 nm. Wile-type *E. coli* PHL628 was used as a negative control. (C) *p*-NPB hydrolysis assay to measure esterase activity. One unit (U) of enzyme activity was defined as the amount of enzyme that hydrolyzes 1 mmol of *p*-NPB substrate per minute under the assay conditions. All experiments were conducted in triplicates and values represent the mean ± standard error. (D) PCL film depolymerization performance of PCL-D. The reaction was conducted using 5 U of PCL-D and 50 mg of PCL film in 50 mM glycine–NaOH buffer (pH 9). (E) Time-course (0 h, 4 h, 8 h, 12 h) FE-SEM images of PCL film. Statistical significance was determined by a two-tailed unpaired Student's *t*-test with Welch's correction. $^{**}p < 0.01$.

12 h, generating 1.91 g L^{-1} of 6-HHA with a yield of 0.97 g 6-HHA per g PCL (Fig. 2D), while the negative control did not produce detectable 6-HHA, confirming that the depolymerization activity originated from the surface-displayed FsC. FE-SEM images revealed progressive surface erosion of PCL films during depolymerization (Fig. 2E). At the beginning of the experiment, the surface was smooth and intact, whereas small pores appeared after 4 h. By 8 h, the pores enlarged, cracks began to appear, and the film started to fragment. At 12 h, most of the PCL film had been depolymerized, with a weight loss of 95.8%. These results confirmed that PCL-D retained high catalytic activity toward PCL depolymerization and effectively catalyzed its hydrolysis at the polymer–liquid interface. In all, our results demonstrated the successful construction of a depolymerization module in the biocatalyst, which was capable of efficiently depolymerizing PCL.

Bioconversion module: functional expression of 6-HHA to adipic acid pathway

To establish a bioconversion pathway for upcycling the PCL depolymerization product 6-HHA to adipic acid, we constructed a two-step pathway by expressing the 6-HHA dehydrogenase (ChnD) and 6-oxohexanoic acid dehydrogenase (ChnE) from *Acinetobacter* sp. SE19,[28] yielding the strain PCL-U (Fig. 3A). In this pathway, ChnD first oxidizes 6-HHA to 6-oxohexaonic acid (6-OHA), which is further oxidized to adipic acid by ChnE. To validate the bioconversion pathway, PCL-U was incubated with 6-HHA, and adipic acid production was monitored over time. PCL-U completely converted 2.5 g L^{-1} 6-HHA into adipic acid within 7 h (Fig. 3B), confirming the successful establishment of a functional upcycling pathway. Notably, we observed that elevated 6-HHA concentrations substantially inhibited cell growth and bioconversion efficiency. At 5 g L^{-1} 6-HHA, PCL-U achieved only ~45% conversion after 22 h, with cell growth reduced by 40% compared to 2.5 g L^{-1} 6-HHA conditions (Fig. S3A). At 10 g L^{-1} of 6-HHA, cell growth was completely inhibited, and no conversion was observed (Fig. S3B). The inhibition effect may be attributed to the toxicity of 6-HHA, which impaired cell metabolism and activity of the bioconversion pathway. Previous study have also reported that 6-HHA concentration over 2.64 g L^{-1} inhibited cell growth and metabolism.[28] These findings highlight that our targeted approach of simultaneous depolymerization and conversion,

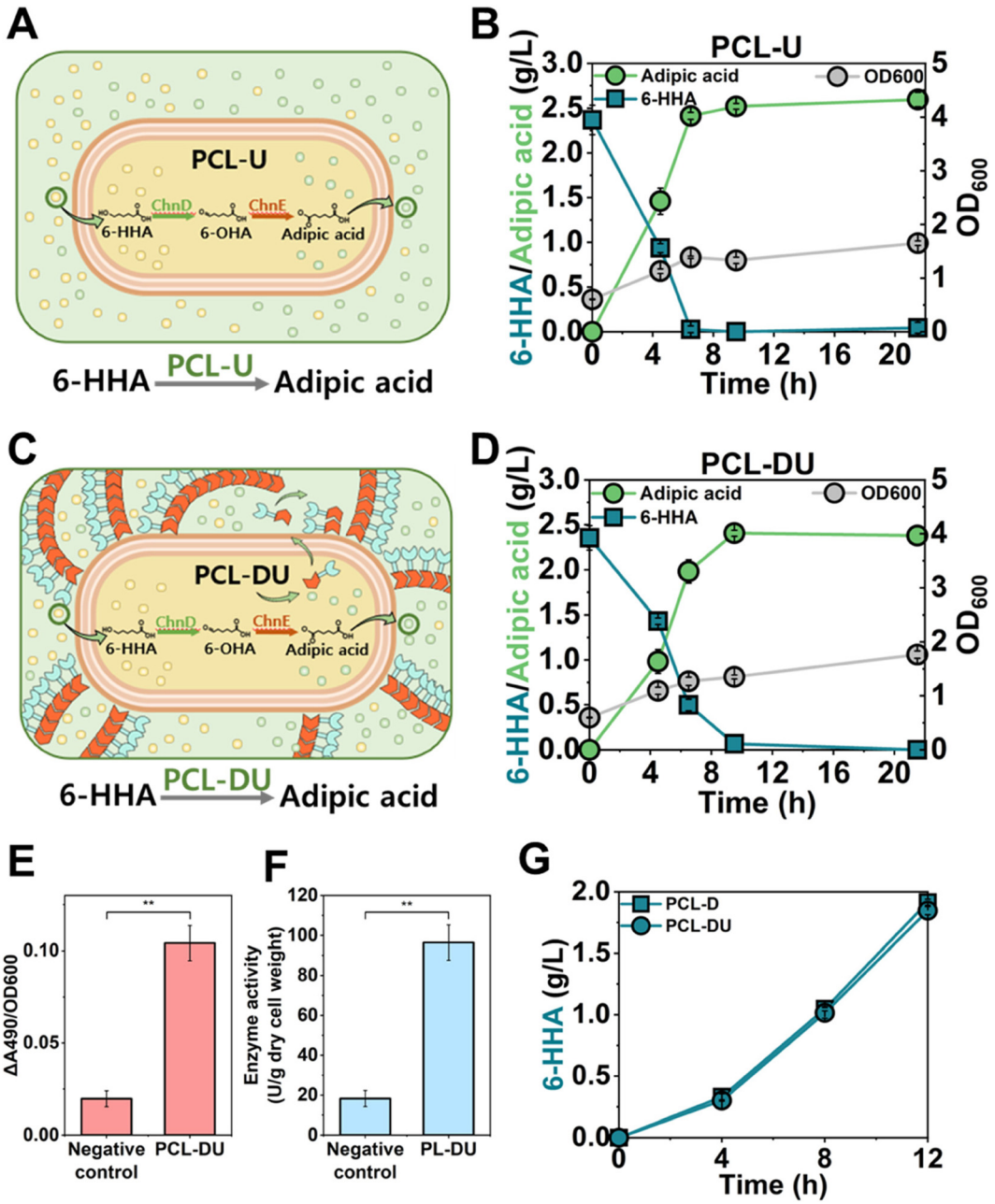

Fig. 3 Construction and characterization of 6-HHA to adipic acid bioconversion module in PCL-U and PCL-DU biocatalysts. (A) Schematic diagram of PCL-U. Bioconversion module is expressed in PCL-U, in which ChnD and ChnE enzymes are expressed to sequentially oxidize 6-HHA into 6-OHA and finally adipic acid. (B) Conversion of 6-HHA into adipic acid by PCL-U biocatalyst. (C) Schematic diagram of PCL-DU in bioconversion of 6-HHA to adipic acid. (D) Performance of PCL-DU in upcycling 6-HHA to adipic acid. (E) Congo red binding assay of PCL-DU. Wile-type *E. coli* PHL628 was used as a negative control. (F) *p*-NPB activity assay of PCL-DU. One unit (U) of enzyme activity was defined as the amount of enzyme that hydrolyzes 1 mmol of *p*-NPB substrate per minute under the assay conditions. (G) PCL film depolymerization performance of PCL-D and PCL-DU. The reaction was conducted using 5 U of PCL-D and 50 mg of PCL film in 50 mM glycine–NaOH buffer (pH 9). All measurements were conducted in triplicate. All experiments were conducted in triplicates and values represent the mean ± standard error. Statistical significance was determined by a two-tailed unpaired Student's *t*-test with Welch's correction. $^{**}p < 0.01$.

where 6-HHA is immediately consumed as it forms, could be an important and effective strategy to mitigate substrate toxicity and enhance overall upcycling efficiency.

We next introduced the bioconversion pathway into the PCL-D strain to integrate the two modules into a single microbial catalyst PCL-DU (Fig. 3C). This engineered biocatalyst couples curli-displayed FsC for extracellular PCL depolymerization with the intracellular ChnD/ChnE pathway for conversion of the intermediate 6-HHA into adipic acid. The functionality of bioconversion module in PCL-DU was well retained

after integration with the depolymerization module. PCL-DU completely converted 2.5 g L^{-1} of 6-HHA into adipic acid within 10 h and achieved a yield of 1.01 ± 0.07 g adipic acid per g 6-HHA, comparable to that by PCL-D (1.10 ± 0.08 g adipic acid per g 6-HHA) (Fig. 3D). Importantly, introduction of the bioconversion module into PCL-D did not compromise depolymerization efficiency. PCL-DU formed robust curli fibers, exhibiting a 5.3-fold increase in congo red binding relative to the control (Fig. 3E), and maintained high enzyme activity of 96.43 ± 8.82 U g^{-1} dry cell weight toward *p*-NPB (Fig. 3F). The depolymerization performance of PCL-DU was further evaluated using PCL films in glycine–NaOH buffer and compared with that of PCL-D. PCL-DU degraded the PCL film efficiently, generating 1.85 ± 0.03 g L^{-1} of 6-HHA within 12 h at a rate of 0.15 g 6-HHA per L per h, and achieving a weight loss of 90.5% (Fig. 3G). These performance parameters were comparable to PCL-D, which produced 1.91 ± 0.03 g L^{-1} of 6-HHA and reached a 93.7% weight loss over the same period. In all, these results confirmed the effective integration of the depolymerization and bioconversion modules and the successful construction of the dual-functional biocatalyst PCL-DU.

Simultaneous depolymerization and upcycling of PCL to adipic acid

After confirming the functionality of both depolymerization and bioconversion modules of PCL-DU, we next investigated whether this biocatalyst could achieve simultaneous PCL depolymerization and upcycling in a one-pot system (Fig. 4A). To this end, 5 U of PCL-DU biocatalyst was incubated with 50 mg of PCL film in YESCA medium supplemented with antibiotics at 37 °C with shaking at 250 rpm. PCL-DU completely depolymerized the PCL film within 12 h, concurrently converting it into adipic acid at a rate of 0.15 ± 0.02 g L^{-1} h^{-1} with little intermediate accumulation (Fig. 4B).

To determine the optimal reaction conditions for PCL upcycling, we evaluated the performance of PCL-DU under varying incubation temperatures (30 °C, 37 °C, and 42 °C) and shaking speeds (0, 60, 100, and 250 rpm). The production of adipic acid and 6-HHA varied under different temperature and aeration conditions (Fig. 4C). First, PCL upcycling efficiency, as indicated by conversion rate for adipic acid production, increased as temperature was raised from 30 °C to 37 °C (Fig. 4D). For example, at 60 rpm, the conversion rate increased from 0.09 ± 0.02 g adipic acid per L per d to 0.12 ± 0.02 g adipic acid per L per d ($p < 0.05$, two-tailed unpaired *t*-test) and at 100 rpm, it increased from 0.22 ± 0.02 g adipic acid per L per d to 0.30 ± 0.02 g adipic acid per L per d ($p < 0.05$, two-tailed unpaired *t*-test). Increasing the temperature further to 42 °C did not lead to any improvement in conversion efficiency. In addition, accumulation of 6-HHA was found to be lowest at 37 °C among all the temperature conditions (Fig. 4C and Fig. S4). At 37 °C and 100 rpm or 250 rpm, only 7–8% of the final products remained as 6-HHA, whereas at 30 °C or 42 °C, 19–25% and 19–23% remained unconverted, respectively, indicating sub-optimal metabolic activity of the PCL-DU cells.

The efficiency of the 6-HHA to adipic acid bioconversion module was found to be sensitive to aeration, with increased oxygen levels enhancing the conversion efficiency. Under static conditions, accumulation of 6-HHA was observed across all temperatures. For example, 85% and 91% of the final products remained as 6-HHA at 30 °C and 37 °C respectively (Fig. 4E), suggesting the low activity of bioconversion module. These observations suggest that oxygen availability was a limiting factor for the ChnD/ChnE-catalyzed dehydrogenation reactions under low agitation conditions. Both ChnD and ChnE depend on NAD^+-dependent redox cycling, which requires continuous regeneration of the oxidized cofactor to sustain catalytic activity. Under static conditions, NAD^+ regeneration is limited due to lack of sufficient oxygen as the terminal electron acceptor,[32] which could stall the oxidative conversion of 6-HHA to adipic acid. In contrast, increasing the shaking speed substantially increased the conversion of 6-HHA into adipic acid. For example, at 37 °C, under 100 rpm and 250 rpm, near-complete conversion of 6-HHA to adipic acid was achieved, with 92% and 93% of the products present as adipic acid, respectively (Fig. 4E), suggesting that aeration is essential for the bioconversion module. The similar conversion efficiency under 100 rpm and 250 rpm conditions also suggested that oxygen level was sufficient at 100 rpm for the PCL-DU biocatalyst. Based on these results, 37 °C and 100 rpm were selected as the optimal conditions for one-pot PCL conversion for the following investigations.

PCL upcycling in fed-batch processes

Fed batch operation is expected to sustain catalytic activity over extended reaction time, improve overall conversion efficiency, and enhance production titter. Therefore, we conducted fed-batch experiments to assess performance of the PCL-DU biocatalyst and optimized operational conditions for PCL upcycling under application-relevant scenarios. We first investigated the effect of biocatalyst loading by initiating fed-batch PCL upcycling experiment with different initial cell densities, including OD_{600} 5, 10, and 20. After 5 days, PCL-DU with starting OD_{600} = 5 produced 10.86 ± 2.18 g L^{-1} of adipic acid, while experiments with higher initial cell densities showed no substantial improvement (Fig. S5). Therefore, all subsequent experiments were conducted using an initial OD_{600} of 5 of PCL-DU. The fed-batch experiment was initiated with PCL-DU cells with 0.8 mM IPTG to induce enzyme expression at the start of the reaction. Fresh 10× concentrated medium was periodically supplemented every 24 h, as detailed in Methods. PCL-DU effectively depolymerized PCL films under fed-batch conditions, exhibiting high upcycling efficiency and producing 14.82 ± 1.00 g L^{-1} of adipic acid over 216 hours, with an average production rate of 1.65 ± 0.11 g adipic acid per L per d (Fig. 5A). Overall, PCL-DU depolymerized 88% of the supplied PCL film, yielding 0.89 ± 0.01 g adipic acid per g PCL during the experimental time frame. There was no detectable accumulation of 6-HHA intermediate, suggesting efficient bioconversion pathway and PCL upcycling by PCL-DU.

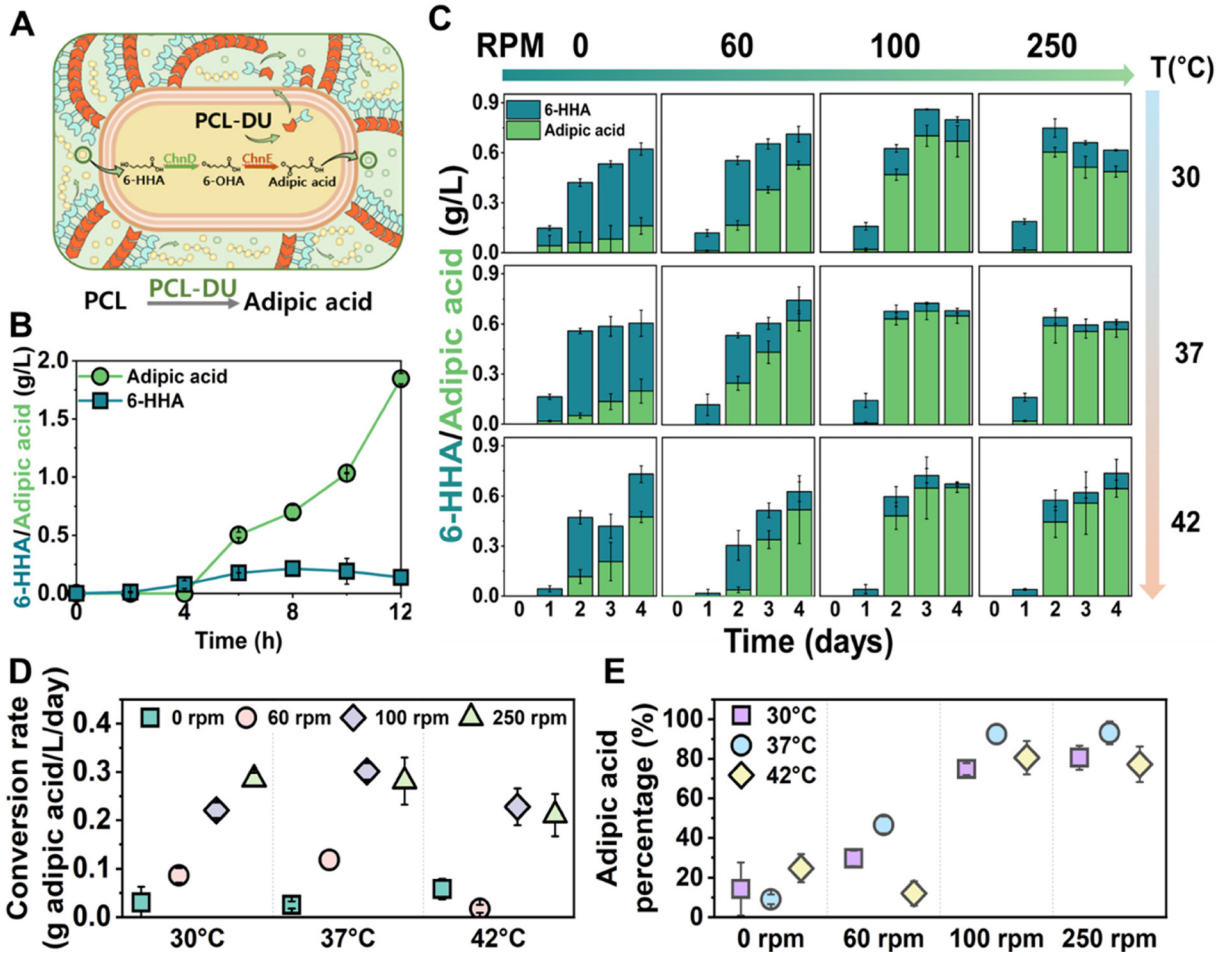

Fig. 4 Simultaneous PCL depolymerization and upcycling using PCL-DU biocatalyst. (A) Schematic diagram of PCL-DU in depolymerization and conversion of PCL to adipic acid. (B) Time-course PCL upcycling by PCL-DU. The reaction was conducted using 5 U of PCL-DU and 50 mg of PCL film in YESCA medium with antibiotics at 37 °C with shaking at 250 rpm. (C) Characterization of PCL-DU biocatalytic activity under reaction conditions at different agitation speeds (0–250 rpm) and temperatures (30–42 °C). 40 mg of PCL film was used for each reaction. (D) Conversion rates of PCL-DU under different temperatures and shaking speeds. The conversion rate was calculated based on the adipic acid production by day 2. (E) Adipic acid mass fraction among total products at day 2 under different temperatures and shaking speeds. All experiments were conducted in triplicates and values represent the mean ± standard error.

We next evaluated whether IPTG and antibiotics are required during the fed-batch PCL upcycling process, considering that the use of inducers and antibiotics may pose cost and regulatory challenges in large-scale applications.[33,34] To this end, PCL-DU was tested under two different conditions: (1) without antibiotics and with IPTG, and (2) pre-induced biocatalyst without further addition of IPTG or antibiotics, while maintaining the same 10× concentrated YESCA feeding every 24 h (Fig. 5B and C). Notably, high catalytic activity was maintained even in the absence of antibiotics, yielding 14.66 ± 0.58 g L^{-1} of adipic acid with a production rate and yield of 1.63 ± 0.06 g adipic acid per L per d and 0.87 ± 0.01 g adipic acid per g PCL, respectively (Fig. 5D). Although antibiotics were absent, the PCL-DU cells might have retained the expression plasmids to sustain the depolymerization and bioconversion modules, allowing the biocatalyst to sustain catalytic activity over the course of reaction. Furthermore, pre-induced PCL-DU without additional inducer or antibiotics in the reaction achieved an adipic acid titer of 12.07 ± 0.07 g L^{-1}, corresponding to approximately 80% of that obtained with PCL-DU supplemented with both IPTG and antibiotics (Fig. 5D). These results suggest that early induction may be sufficient to sustain catalytic activity throughout the entire reaction process, eliminating the need for IPTG or antibiotics in the operational phase. Operating without antibiotics and IPTG can further reduce overall process costs, simplifies downstream processing, and alleviates regulatory burdens associated with antibiotic use in large-scale biocatalytic plastic depolymerization and upcycling.[34,35] Taken together, these results show that PCL-DU maintained robust catalytic activity even under inducer- and antibiotic-free conditions without intermediate accumulation, supporting its potential for industrial plastic upcycling applications.

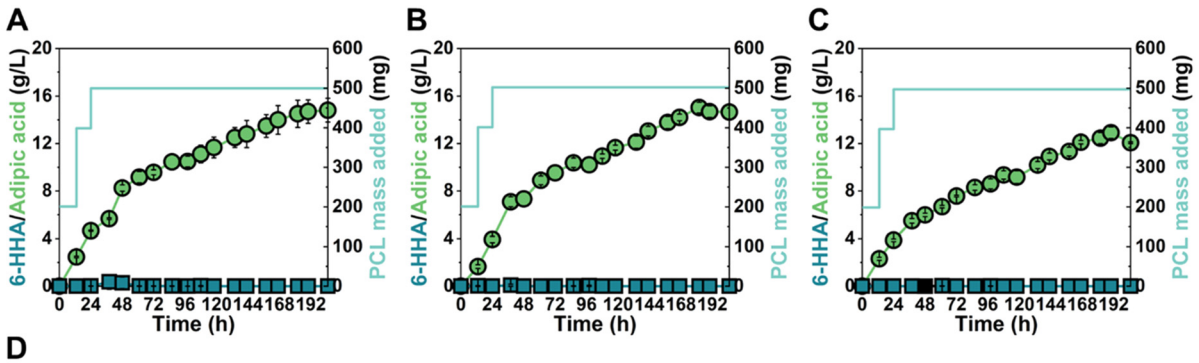

D

Figure	Conditions	Titer (g/L)	Productivity (g adipic acid/L/d)	Yield (g adipic acid/g PCL)
a	OD_{600}=5 cell w. antibiotics and IPTG	14.82±1.01	1.65±0.11	0.89±0.01
b	OD_{600}=5 cell w/o. antibiotics and w. IPTG	14.66±0.58	1.63±0.06	0.87±0.01
c	Pre-induced OD_{600}=5 of PCL-DU w/o. antibiotics and w/o. IPTG	12.07±0.07	1.34±0.01	0.83±0.00

Fig. 5 Fed-batch PCL valorization using PCL-DU biocatalyst. (A) Time-course depolymerization and upcycling of PCL using the PCL-DU. PCL-DU cells (OD_{600} = 5) were incubated in YESCA medium supplemented with antibiotics, 0.8 mM IPTG, and 200 mg of PCL film, with 10× concentrated YESCA medium and antibiotics supplemented every 24 h. (B) Time-course upcycling of PCL using the PCL-DU with IPTG but without antibiotics. PCL-DU cells (OD_{600} = 5) were incubated in YESCA medium with 0.8 mM IPTG and 200 mg of PCL film, with 10× concentrated YESCA medium supplemented every 24 h. (C) Time-course upcycling of PCL using pre-induced PCL-DU biocatalyst without IPTG and antibiotics. PCL-DU cells were induced, washed, and then incubated in YESCA medium containing 200 mg of PCL film, with 10× concentrated YESCA medium supplemented every 24 h. In all experiments, an additional 200 mg and 100 mg of PCL film were added on day 1 and day 2, respectively. (D) Fed-batch performance parameters of the PCL-DU biocatalyst under different operational conditions. All experiments were conducted in triplicates and values represent the mean ± standard error.

Open-loop upcycling of post-consumer PCL to nylon-6,6

After demonstrating efficient one-pot depolymerization and upcycling of PCL film by the engineered PCL-DU strain, we proposed that this microbial catalyst would be suitable for a biocatalytic-chemical process for upcycling of real-world post-consumer PCL to new products such as nylon-6,6. In this regard, we demonstrate here an open-loop valorization of PCL product with biocatalytic depolymerization and conversion PCL to adipic acid by PCL-DU strain and subsequent recovery of adipic acid and synthetic into nylon-6,6 (Fig. 6A). A 3D-printed PCL product (3.17 × 5.08 cm, 5 g) was fabricated using a commercial PCL filament (Fig. S6) and incubated with PCL-DU, with 10× concentrated YESCA medium supplemented every 24 h. The biocatalyst effectively depolymerized 48% of the 3D-printed PCL product within 10 days, producing 9.63 g L^{-1} of adipic acid with a productivity of 0.96 g adipic acid per L per d and overall yield of 0.81 g adipic acid per g PCL (Fig. 6B). To investigate the observed plateau after day 9, the biocatalyst was harvested at day 10 and its residual activity was measured. The harvested biocatalyst exhibited negligible enzymatic activity, suggesting that loss of biocatalyst activity was a primary factor limiting further depolymerization. A minor accumulation of 6-HHA (1.35 g L^{-1}) was observed, indicating that the bioconversion module was the rate-limiting step in the current system. This limitation could potentially be alleviated by increasing the expression level of the pathway enzymes, engineering ChnD/ChnE to enhance catalytic efficiency, or improving cellular uptake of 6-HHA to enhance intermediate transformation flux.

We then demonstrated successful synthesis of nylon-6,6 from the adipic acid produced from PCL (Fig. 6A). After the PCL depolymerization and conversion reaction catalyzed by PCL-DU, the culture medium was treated with activated carbon (GAC) and adjusted to pH < 2, after which adipic acid was recovered by crystallization. Adipic acid was recovered from the culture medium, with a high purity of 98% as determined by differential scanning calorimetry (DSC) analysis (Fig. S7). Then, nylon-6,6 polymer was obtained through chemical polymerization using $SOCl_2$ and HMDA. Commercially available adipic acid was used as the positive control substrate in the same polymerization process for comparison. The spectra of the two nylon-6,6 products obtained were essentially identical (Fig. 6C), both showing a strong match with the nylon-6,6 standard spectrum in the library database (Fig. S8). Characteristic absorption bands of nylon-6,6 were observed in both spectra, including the N–H stretching (~3301 cm^{-1}), C–H stretching (~2930–2850 cm^{-1}), amide I (~1640 cm^{-1}), amide II (~1540 cm^{-1}), and C–N/CH_2 vibrations (1200–1000 cm^{-1}), confirming successful polymerization. The similar chemical composition of the two nylon-6,6 samples was further confirmed by pyrolysis-GC-MS analysis, which produced identical fragmentation patterns and peak distri-

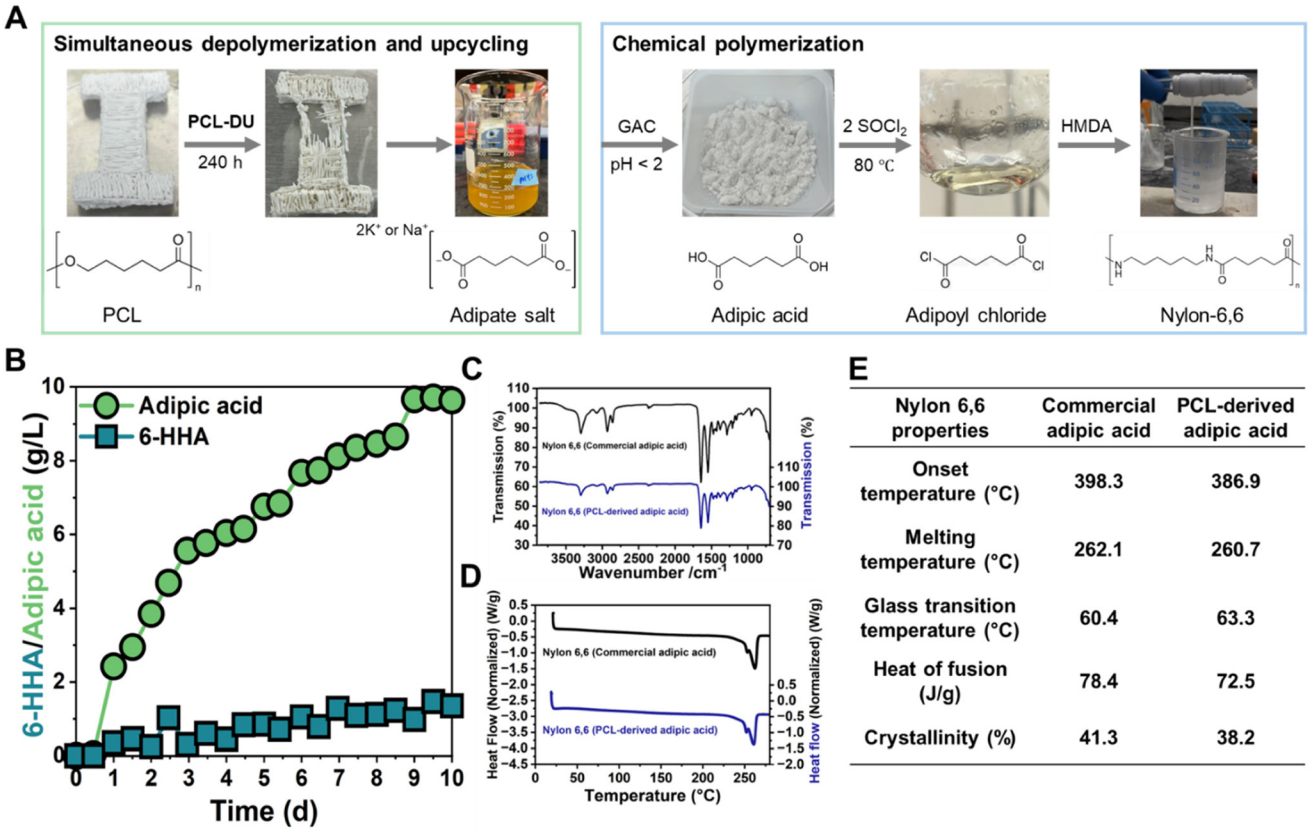

E

Nylon 6,6 properties	Commercial adipic acid	PCL-derived adipic acid
Onset temperature (°C)	398.3	386.9
Melting temperature (°C)	262.1	260.7
Glass transition temperature (°C)	60.4	63.3
Heat of fusion (J/g)	78.4	72.5
Crystallinity (%)	41.3	38.2

Fig. 6 Open-loop upcycling of post-consumer PCL product by PCL-DU biocatalyst coupled with downstream chemical polymerization. (A) Schematic of the open-loop PCL upcycling process. Post-consumer PCL products were depolymerized and converted into adipic acid by PCL-DU. The recovered adipic acid was subsequently utilized to synthesize nylon-6,6. (B) Time-course depolymerization and upcycling of post-consumer PCL by the PCL-DU biocatalyst. Post-consumer PCL product was incubated with PCL-DU biocatalyst at 37 °C, with 10× concentrated YESCA medium and antibiotics supplemented every 24 h. (C) IR spectrum of nylon-6,6 synthesized with commercial and PCL-derived adipic acid. (D) DSC thermal analysis of nylon-6,6 produced from commercial adipic acid and PCL-derived adipic acid. The polymer was scanned from 20 °C to 275 °C at a rate of 10 °C per minute. (E) Thermal properties of nylon-6,6 synthesized with commercial and PCL-derived adipic acid.

butions in the mass spectra (Fig. S9) and consistent retention times and peak intensities in the chromatographic profiles (Fig. S10). After confirming their compositional equivalence, the thermal properties of the nylon-6,6 samples were analyzed. The thermal properties of nylon-6,6 synthesized with PCL-derived adipic acid were comparable to those obtained from commercial adipic acid (Fig. 6D and E, and Fig. S11). Both nylon-6,6 samples exhibited nearly identical melting temperatures (262.1 °C and 260.7 °C) determined by TGA, and similar glass transition temperatures (60.4 °C and 63.3 °C), suggesting that the adipic acid purified from PCL upcycling functioned equivalently to the commercial adipic acid in nylon-6,6 synthesis. These results demonstrate the feasibility of open-loop biocatalytic upcycling of PCL coupled with chemical polymerization to produce the valuable product nylon-6,6.

Conclusion

The dual-functional microbial catalyst PCL-DU developed here establishes a new class of biocatalytic platforms capable of overcoming major obstacles in transforming end-of-life plastics into valuable products. By integrating a curli displayed plastic depolymerizing enzyme with an intracellular biotransformation pathway, PCL-DU enabled efficient one-pot valorization of post-consumer PCL into high-value chemical adipic acid under mild conditions, without the need for costly enzyme purification or complex intermediate separation. Notably, we demonstrated efficient upcycling of a real-world 3D-printed PCL product to adipic acid with high yield. The recovered adipic acid was subsequently used to synthesize nylon-6,6, thereby completing a full open-loop upcycling pathway from waste plastic to industrial material.

The presented biocatalytic platform advances the development of economically viable and scalable plastic upcycling technologies, by eliminating protein purification steps, enabling direct conversion of depolymerized intermediates, alleviating substrate inhibition, and enhancing overall conversion efficiency and carbon recovery. Moreover, it is noteworthy that the platform is inherently modular: by reprogramming curli-displayed enzymes and tailoring intracellular biocatalytic pathways for desirable biotransformation, new microbial

catalysts could be developed for simultaneous depolymerization and upcycling of diverse plastics beyond PCL. Future work will further optimize the bioconversion pathway enhance the final product yield, and develop genome-integrated, antibiotic-free, and inducer-free biocatalysts to ensure biocatalyst stability, improve cost-effectiveness, and minimize potential environmental risks for scalable industrial plastic upcycling applications. In all, this study establishes a foundational strategy to advance sustainable biomanufacturing that valorizes plastic waste as a carbon feedstock and addresses the grand challenge of plastic pollution within a circular bioeconomy framework.

Author contributions

N. W., Y.-S. J. and S. M. K. designed research. S. M. K., Y. S. and R. J. performed research. S. M. K. and L. T. analyzed data. L. Z. and J. W. S. analyzed polymers. S. M. K., L. Z., Y.-S. J., and N. W. wrote the paper. All authors read and approved the paper.

Conflicts of interest

The authors declare no competing interests.

Data availability

All data supporting the findings of this study are available within the article, as well as the supplementary information (SI). All data are available from the corresponding author upon request.

Supplementary information: plasmid maps (Fig. S1), congo red assay for PCL-D and PCL-DU (Fig. S2), conversion of 6-HHA into adipic acid using PCL-U (Fig. S3), fraction of 6-HHA among total soluble product at day 2 under different conditions (Fig. S4), soluble product concentration after 5 days incubation with different initial cell densities of PCL-DU (Fig. S5), time-course degradation of post-consumer PCL product (Fig. S6), differential scanning calorimetry analysis of recovered adipic acid (Fig. S7), infrared spectrum of nylon-6,6 (Fig. S8), pyrolysis-GC-MS spectrometry of nylon-6,6 (Fig. S9), overlay of pyrolysis-GC-MS spectrometry of nylon-6,6 (Fig. S10), thermogravimetric analysis of nylon-6,6 (Fig. S11), primers used in the study (Table S1). See DOI: https://doi.org/10.1039/d6gc00678g.

Acknowledgements

This work was supported by National Science Foundation (CBET-2154345). The authors thank Dr Neel S. Joshi at Northeastern University for kindly sharing the plasmid pBbE1a and *E. coli* PHL628 strain. FE-SEM, TGA, and DSC analysis were carried out in part in the Materials Research Laboratory Central Research Facilities, University of Illinois.

References

1 Y. Tang, Y. Liu, Y. Chen, W. Zhang, J. Zhao, S. He, C. Yang, T. Zhang, C. Tang and C. Zhang, *Sci. Total Environ.*, 2021, **766**, 142572.
2 P. Redondo-Hasselerharm, G. Gort, E. Peeters and A. Koelmans, *Sci. Adv.*, 2020, **6**, eaay4054.
3 B. Boots, C. W. Russell and D. S. Green, *Environ. Sci. Technol.*, 2019, **53**, 11496–11506.
4 J.-G. Rosenboom, R. Langer and G. Traverso, *Nat. Rev. Mater.*, 2022, **7**, 117–137.
5 M. Labet and W. Thielemans, *Chem. Soc. Rev.*, 2009, **38**, 3484–3504.
6 M. A. Woodruff and D. W. Hutmacher, *Prog. Polym. Sci.*, 2010, **35**, 1217–1256.
7 V. Guarino, G. Gentile, L. Sorrentino and L. Ambrosio, *Encyclopedia of polymer science and technology*, 2002, pp. 1–36.
8 D. Chen, J. Bei and S. Wang, *Polym. Degrad. Stab.*, 2000, **67**, 455–459.
9 C. X. Lam, S. H. Teoh and D. W. Hutmacher, *Polym. Int.*, 2007, **56**, 718–728.
10 M. González Petit, Z. Correa and M. Sabino, *J. Polym. Environ.*, 2015, **23**, 11–20.
11 T. Ishigaki, W. Sugano, A. Nakanishi, M. Tateda, M. Ike and M. Fujita, *Chemosphere*, 2004, **54**, 225–233.
12 G. Suaria, C. G. Avio, A. Mineo, G. L. Lattin, M. G. Magaldi, G. Belmonte, C. J. Moore, F. Regoli and S. Aliani, *Sci. Rep.*, 2016, **6**, 37551.
13 H. Li, H. A. Aguirre-Villegas, R. D. Allen, X. Bai, C. H. Benson, G. T. Beckham, S. L. Bradshaw, J. L. Brown, R. C. Brown and V. S. Cecon, *Green Chem.*, 2022, **24**, 8899–9002.
14 D. K. Barnes, F. Galgani, R. C. Thompson and M. Barlaz, *Philos. Trans. R. Soc., B*, 2009, **364**, 1985–1998.
15 C. Jehanno, J. W. Alty, M. Roosen, S. De Meester, A. P. Dove, E. Y.-X. Chen, F. A. Leibfarth and H. Sardon, *Nature*, 2022, **603**, 803–814.
16 B. Zhu, D. Wang and N. Wei, *Trends Biotechnol.*, 2022, **40**, 22–37.
17 J. Rios, J. Lebeau, T. Yang, S. Li and M. D. Lynch, *Green Chem.*, 2021, **23**, 3172–3190.
18 M. M. Research, *Global Nylon 66 Market: Industry Analysis and Forecast (2023–2029)*, Pune, India, 2024.
19 J. C. Bart and S. Cavallaro, *Ind. Eng. Chem. Res.*, 2015, **54**, 1–46.
20 B. Zhu, Q. Ye, Y. Seo and N. Wei, *Environ. Sci. Technol. Lett.*, 2022, **9**, 650–657.
21 A. Rosato, A. Romano, G. Totaro, A. Celli, F. Fava, G. Zanaroli and L. Sisti, *Polymers*, 2022, **14**, 1850.
22 Y.-R. Oh, Y.-A. Jang, J. K. Song and G. T. Eom, *Biochem. Eng. J.*, 2022, **185**, 108504.

23 K. Shi, J. Jing, L. Song, T. Su and Z. Wang, *Int. J. Biol. Macromol.*, 2020, **144**, 183–189.
24 V. Tournier, S. Duquesne, F. Guillamot, H. Cramail, D. Taton, A. Marty and I. André, *Chem. Rev.*, 2023, **123**, 5612–5701.
25 P. Q. Nguyen, Z. Botyanszki, P. K. R. Tay and N. S. Joshi, *Nat. Commun.*, 2014, **5**, 4945.
26 D. Pawar, M. Rossman and J. Chen, *J. Appl. Microbiol.*, 2005, **99**, 418–425.
27 C. A. Murphy, J. Cameron, S. J. Huang and R. T. Vinopal, *Appl. Environ. Microbiol.*, 1996, **62**, 456–460.
28 Y.-R. Oh, Y.-A. Jang and G. T. Eom, *Enzyme Microb. Technol.*, 2024, **181**, 110521.
29 D. R. Smith, J. E. Price, P. E. Burby, L. P. Blanco, J. Chamberlain and M. R. Chapman, *Biomolecules*, 2017, **7**, 75.
30 M. Khorramnezhad, B. Akbari, M. Akbari and M. Kharaziha, *Colloids Surf., B*, 2021, **200**, 111582.
31 G. Hidalgo, X. Chen, A. G. Hay and L. W. Lion, *Appl. Environ. Microbiol.*, 2010, **76**, 6939–6941.
32 S. J. Berrıos-Rivera, G. N. Bennett and K.-Y. San, *Metab. Eng.*, 2002, **4**, 217–229.
33 G. L. Rosano and E. A. Ceccarelli, *Front. Microbiol.*, 2014, **5**, 172.
34 R. d. G. Ferreira, A. R. Azzoni and S. Freitas, *Biotechnol. Biofuels*, 2018, **11**, 81.
35 J. L. Martinez, *Environ. Pollut.*, 2009, **157**, 2893–2902.